https://doi.org/10.5194/amt-2020-238
Preprint. Discussion started: 7 July 2020

Atmospheric Measurement Techniques Discussions

manuscript submitted to *Atmospheric Measurement Techniques*

Assimilation of lidar planetary boundary layer height observations.

Andrew Tangborn[1], Belay Demoz[1,2], Brian J. Carroll[2], Joseph Santanello[3]and Jeffrey L. Anderson[4]

[1]JCET, UMBC, Baltimore, MD, USA
[2]Dept. of Physics, UMBC, Baltimore, MD, USA
[3]Laboratory for Hydrology, NASA GSFC, Greenbelt, MD, USA
[4]National Center for Atmospheric Research, Boulder, CO, USA

Corresponding author: Andrew Tangborn, tangborn@umbc.edu

https://doi.org/10.5194/amt-2020-238
Preprint. Discussion started: 7 July 2020

Atmospheric Measurement Techniques Discussions

Abstract

Lidar backscatter and wind retrievals of the planetary boundary layer height (PBLH) are assimilated into 22 hourly forecasts from the NASA Unified - Weather and Research Forecast (NU-WRF) model during the Plains Elevated Convection Convection at Night (PECAN) campaign on July 11, 2015 in Greensburg, Kansas, using error statistics collected from the model profiles to compute the necessary covariance matrices. Two separate forecast runs using different PBL physics schemes were employed, and comparisons with 5 independent sonde profiles were made for each run. Both of the forecast runs accurately predicted the PBLH and the state variable profiles within the planetary boundary layer during the early morning, and the assimilation had little impact during this time. In the late afternoon, the forecast runs showed decreased accuracy as the convective boundary layer developed. However, assimilation of the doppler lidar PBLH observations were found to improve the temperature, water vapor and velocity profiles relative to independent sonde profiles. The computed forecast error covariances between the PBLH and state variables were found to rise in the late afternoon, leading to the larger improvements in the afternoon. This work represents the first effort to assimilate PBLH into forecast states using ensemble methods.

1 Introduction

The planetary boundary layer (PBL) plays an important role in both weather and climate. This layer is where the Earth's surface interacts with the atmosphere, exchanging heat, moisture and pollutants. The PBL height (PBLH) is central to these interactions and is controlled by the energy flux from the surface. Under certain conditions during daytime it defines the convective boundary layer (CBL) and during nighttime it is the stable (non-convective) boundary layer (SBL). Trace gases and aerosols emitted from the surface are rapidly transported within this layer by turbulent atmospheric motion, and transfer of energy and mass into the free troposphere occurs across an interfacial layer at the top of the PBL. The PBLH is fundamental to weather, climate, atmospheric turbulence and pollution through its role in land-atmosphere interactions and mediation of Earth's water and energy cycles (Santanello et al. 2018) and its impact on convection in the troposphere, which is generally initiated within the boundary layer and then penetrates the top (Hong and Pan, 1998; Browning, et al. 2007). Thus, accurate knowledge of the PBLH is essential for both weather and climate forecasting.

https://doi.org/10.5194/amt-2020-238
Preprint. Discussion started: 7 July 2020

Atmospheric Measurement Techniques Discussions

The PBLH is defined by thermodynamic properties such as a temperature inversion or hydrolapse which can be measured by radiosonde. Alternatively the drop off in aerosol concentration that occurs across the top of the PBL is used, since aerosols are well mixed throughout the PBL (Hicks, et al., 2019). Atmospheric models rely on parameterization schemes to define the structure of the PBL and compute PBLH. These are generally either local mixing schemes that use local turbulent kinetic energy (TKE, Janjic, 1994) or flux schemes (Hong and Pan, 1996). Generally, these PBL parameterizations have systematically higher PBLH relative to observed values (Hegarty et al., 2018), and also have difficulties modeling the growth of the convective layer during the morning. These varying and distinct definitions of PBLH across models and observations remain a challenge in terms of utilizing both for process understanding or model evaluation/development.

Observations of PBLH are traditionally made by radiosonde measurements, which have high vertical resolution but are expensive to launch frequently and are thus limited to special experiments and/or ill-timed launches (*e.g.* 00/12Z National Weather Service launches) with respect to the convective and stable PBL development. Likewise, spaceborne measurements of the lower troposphere from passive and active instruments (with the exception of Global Positioning System Radio Occultation (GPSRO), Ao, et al. 2008) are severely limited in vertical, spatial, and/or temporal resolution (Wulfmeyer et al. 2015). Ground based measurement of PBLH has been proposed for an extensive network of ceilometers by adding to the functionality of instruments that were designed for measuring cloud heights [Hicks et al., 2016]. The ceilometer measures the time required for a laser pulse to return to a receiver, from which the height of the scattering is determined. The intensity of the backscatter is correlated with the density of aerosols at a given height and the PBLH is inferred from the location of the maximum negative gradient of the backscatter intensity. Several algorithms employ wavelet transforms to identify the location of the negative gradient (e.g. Brooks, 2003; Knepp, *et al.*, 2017), which relies on finding the wavelet dilation that is large enough to be distinct from noise and small-scale gradients in the backscatter profile. This existing network of ceilometers could be used to create a relatively dense network of frequent PBLH observations, as was recommended by the 2009 study from the National Research Council (NRC, 2009) and the Thermodynamic Profiling Technologies Workshop (NCAR, 2012).

https://doi.org/10.5194/amt-2020-238
Preprint. Discussion started: 7 July 2020

Atmospheric Measurement Techniques Discussions

The lidar observations used in this study were taken at the PECAN site in Greensburg, Kansas. The data is from a commercial Doppler lidar owned and operated by the University of Maryland, Baltimore County (Delgado et al., 2016). This lidar operates at an infrared wavelength, and hence receives its strongest backscattered signal within the aerosol-laden PBL and is often below the noise floor above the PBL. The Doppler shift of the backscattered signal is used to calculate wind speed as a function of range, which can then be used to produce a multitude of wind and turbulence variables useful for PBL characterization (e.g. vertical velocity variance and signal-to-noise ratio variance). The PBLH algorithm applied for this study combines several such aerosol and wind variables for PBLH measurement and was described at length in Bonin et al. (2018). Additional lidar parameters and the application of the algorithm to PECAN data were presented in Carroll et al. (2019). Each PBLH measurement was made from a repeating 25-minute lidar scan cycle.

The question remaining is how to assimilate these observations into a numerical weather prediction (NWP) model. PBLH is a diagnostic variable in NWP parameterized physics models. This means any correction to PBLH will be lost during the model forecast unless the PBLH height observation is used to correct state variables such as temperature and moisture. This could be done either by creating an adjoint of the PBL parameterization scheme, or through the use of an ensemble Kalman filter which would determine the error covariances between PBLH and state variables in the model. The structure of the covariance, and how the state variables are changed by assimilating PBLH, will depend on which PBL scheme is used. We will show how such a system could work by conducting a posteriori lidar PBLH observation impact experiments using forecast fields from a NASA Unified - Weather and Research Forecast (NU-WRF, Lidard-Peters, 2015) model runs for one day during the Plains Elevated Convection at Night (PECAN) campaign on July 11, 2015. The assimilation is done on 22 hourly WRF forecast fields throughout the day without cycling the analysis fields back into the model with two different PBL parameterizations. In this paper, we demonstrate a new and promising method that uses the relative lidar-based aerosol backscatter and wind derived PBLH to correct model forecasted state variables. The purpose here is to show how ensemble computed error covariance can transfer observational information from PBLH to the state variable profiles.

https://doi.org/10.5194/amt-2020-238
Preprint. Discussion started: 7 July 2020

Atmospheric Measurement Techniques Discussions

2 Methodology

The assimilation methodology is based on the ensemble Kalman filter (EnKF)(Evensen, 2009), where the analysis state is the estimate with the minimum estimated errors, relative to the given error statistics. It differs from the EnKF in that the analysis is not used as an initial state for the next model forecast. Rather, two existing one day NU-WRF forecasts, with different PBL physics schemes, are used when lidar measurements are available at a single location. These forecasts were produced as a part of the PECAN campaign in 2015, and we resuse them here to demonstrate the assimilation algorithm that we have developed. These were not ensemble forecasts so we cannot build a standard ensemble Kalman filter from them. Instead we use Ensemble Optimal Interpolation (EnOI), we use profiles from neighboring model gridpoints to obtain and estimate of error statistics (Oke, *et al.*, 2010; Keppenne, *et al.*, 2014). This approach will allow for the construction of the vertical component of covariance, which is needed in order to understand how PBLH can be used to correct atmospheric profiles through the use of profile and PBLH statistics. We use profiles from nearby model grid points and have tested the system with varying numbers of grid points in the ensemble. An ensemble Kalman filter would likely give different covariance information, but the basic relationship between the state variable profiles and the PBLH are determined by the model in the same manner here.

The two NU-WRF simulations use the Mellor–Yamada–Janjic (MYJ)[Mellor and Yamada, 1974, 1982; Janjic, 2002] and Mellor-Yamada-Nakanishi-Niino level 2.5 (MYNN) [Nakanishi and Niino, 2009] which are local 1.5 and 2.5 order turbulence closure schemes respectively. The PBLH in each of these models is estimated using the total kinetic energy (TKE) method. The NU-WRF forecast state variables are temperature (T), moisture (Q) and velocity (U,V), and we define the forecast vector $\mathbf{x}^f = [T^f\ Q^f\ U^f\ V^f\ (PBLH)^f W^f\ ]$, where we have combined PBLH with the state variables to enable the covariance calculation between them. The forecast runs are initiated from a global reanalysis interpolated to the local domain of 30-48N and 84-110 W, with 220×220 lat/lon and 54 vertical levels. Therefore the state at the initial time has assimilated all of the convential and satellite observations globally. This means that our experiments are all less than 24 hours from the most recent global analysis. We use an ensemble of the 20 × 20 nearest gridpoints, so that all of the ensemble members are within about 30 km of the lidar observations (since the grid spacing is about 3 km). Generally, larger ensembles using

https://doi.org/10.5194/amt-2020-238
Preprint. Discussion started: 7 July 2020

Atmospheric Measurement Techniques Discussions

gridpoints farther away will result in larger forecast error covariance because the geographic variability. So this ensemble size was chosen as a balance between ensemble size and geographic localization. The forecast standard deviation for PBLH on the chosen ensemble was around 27 m at 22 UTC.

The forecast error covariance, $\mathbf{P}^f$ is defined as

$$\mathbf{P}^f = \left\langle (\mathbf{x}^f - \mathbf{x}^t)(\mathbf{x}^f - \mathbf{x}^t)^T \right\rangle \tag{1}$$

where the summation is over the grid points $i = 1, N_{lon}$, $j = 1, N_{lat}$ and $\mathbf{x}^t$ is the (unknown) true state, on the discrete model grid. We only assimilate the observation $y^o = PBLH = H(\mathbf{x}^f)$ where H is the non-linear observation operator. The analysis equation is

$$\mathbf{x}^a = \mathbf{x}^f + \mathbf{K}(y^o - H(\mathbf{x}^f)) \tag{2}$$

where the gain matrix, $\mathbf{K}$ is defined by:

$$\mathbf{K} = \mathbf{P}^f\mathbf{H}^T(\mathbf{H}\mathbf{P}^f\mathbf{H}^T + (\sigma^o)^2)^{-1}, \tag{3}$$

σ^o is the observation error standard deviation supplied with the lidar retrievals, and $\mathbf{H}$ is the linearized observation operator for PBLH. Because the PBLH is related to the state variables via the two PBL physics schemes, determining $\mathbf{H}$ would require linearizing the PBL physics at every analysis time. Instead of this approach, we use the ensemble of profiles from the forecast field locations $\mathbf{x}^f$ and the boundary layer heights $PBLH^f$ to obtain the ensemble estimates:

$$\mathbf{P}^f\mathbf{H}^T \approx \left\langle (\mathbf{x}^f - {\mu_\mathbf{x}}^f)\ (H(\mathbf{x}^f - {\mu_\mathbf{x}}^f))^T \right\rangle \tag{4}$$

and

$$\mathbf{H}\mathbf{P}^f\mathbf{H}^T \approx \left\langle H(\mathbf{x}^f - {\mu_\mathbf{x}}^f)\ (H(\mathbf{x}^f - {\mu_\mathbf{x}}^f))^T \right\rangle \tag{5}$$

where ${\mu_\mathbf{x}}^f$ is the mean forecast state of the ensemble of profiles.

We expect the correlation between the airmass within the PBL and the free troposphere to drop away rapidly, because of limited intereactions between them. We found that this can cause errors in the analysis profiles if error covariance and PBLH is allowed to continue into the troposphere. To reduce these errors we have added an exponential decay starting at the model level closest to the PBLH (k_{PBLH}) to define a vertical localization factor:

$$C_{loc} = exp\left[-\alpha(\frac{k - k_{PBLH}}{k_{PBLH}})^2\right] \tag{6}$$

https://doi.org/10.5194/amt-2020-238
Preprint. Discussion started: 7 July 2020


Atmospheric Measurement Techniques Discussions

where k is the model level and α is an experimentally determined factor. This ensures that the covariance between the PBLH and the state variables becomes small within a couple of model levels into the free troposphere.

This system is solved at each hour using the nearest lidar profile observations in time, and the resulting analysis fields are compared to sonde profiles when the latter are also available. There are 22 analyses (for each forecast run), and 5 times where comparison with sonde profiles are made. We focus on the impact of the assimilation on the state variables T, Q, U and V rather than the PBLH because only the state variables would be retained by a forecast.

3 Results

The NU-WRF simulations, taken from existing forecast runs used for the PECAN campaign (Santanello *et al.*, 2019) are initialized using a National Center for Environmental Prediction (NCEP) Global Forecast System (GFS) reanalysis interpolated to the domain 30-48N and 84-110 W, with 54 vertical levels. The two forecast runs were conducted using MYJ PBL physics (2-22 UTC) and MYNN (2-23 UTC) on July 11, 2015. Lidar PBLH observations were made every 25 minutes on that day in Greensburg, KS (37.6 N, 99.3 W), while balloon soundings were launched from that location 6 times as part of the Plains Elevated Convection At Night (PECAN; Gerts et al. 2017). Figure 1 shows the PBLH during that day and derived from the two NU-WRF forecasts, lidar observations and soundings. We have determined the sounding PBLH using the parcel method, which defines the top as the height where the potential temperature first exceeds the ground temperature. The lidar PBLH (black *, derived using the method reported in Bonin, 2018) closely matches the sonde estimates (green triangles) in the late evening to early morning (2-7 UTC), while it is somewhat lower in the afternoon. The two NU-WRF forecasts differ from the observations depending on the time of day. In the early morning and early afternoon the MYJ forecasts (red triangles) are slightly higher than the observations, then fall behind the rise seen in the lidar observations (there are no sonde measurements to compare to here) before rising much higher than the observations in the late afternoon. The MYNN forecasts (blue squares) are lower than the observations from early morning until early afternoon before rising higher (but not as high as MYJ).

https://doi.org/10.5194/amt-2020-238
Preprint. Discussion started: 7 July 2020

Atmospheric Measurement Techniques Discussions

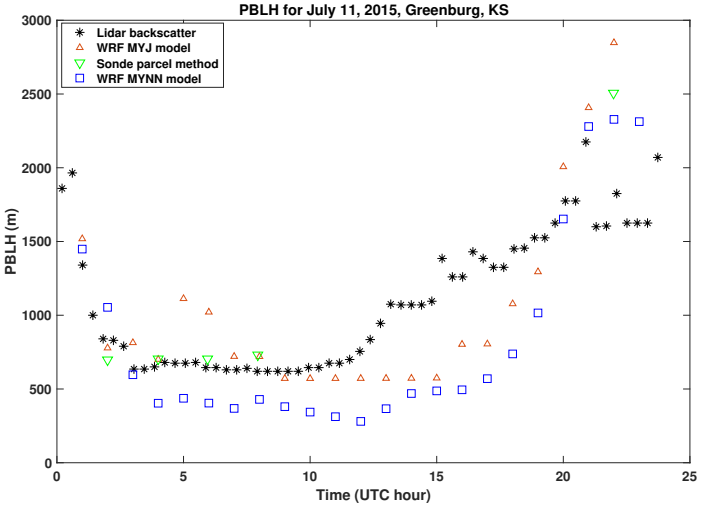

c

Figure 1. PBLH vs UTC time for July 11, 2015 for lidar backscatter (black *), WRF model - MYJ (red triangles), sonde observations using parcel method (green triangles) and WRF model - MYNN (blue squares).

Since we are primarily interested in the impact of the assimilation on state variables within the boundary layer, in Figure 2 we plot the RMS difference between the model and the independent (unassimilated) sonde profiles from the surface to roughly the top of the boundary layer (first 8 levels, or about 800 mb). So for the temperature forecast, the RMS difference would be

$$RMS(t_a) = \left[\frac{1}{8}\sum_{i=1}^{8}(T_i^f - T_i^{sonde})^2\right]^{1/2} \tag{7}$$

where t_a is the analysis time and *ntop* is the model level at the top of the PBL. Figure 2 shows the RMS differences with the sonde profiles throughout the day for the forecasts (blue) and analyses (red) for potential temperature (a), water vapor mixing ratio (b) and the U (c) and V (d) components of velocity. The MYNN profiles are shown by solid lines while the MYJ profiles are dashed lines. During the night (2-9 UTC), the assimilation has very little impact on the potential temperature RMS differences in the early morning (6 and 8 UTC), and the two forecasts have similar accuracy. By late afternoon (22 and 23 UTC, note that the MYJ forecast stops at 22 UTC) the sonde comparisons show that the assimilation reduces RMS differences in the potential temperatures by nearly 50% for MYNN and around 80% for MYJ. The water vapor mixing ratio (b) also has

https://doi.org/10.5194/amt-2020-238
Preprint. Discussion started: 7 July 2020

Atmospheric Measurement Techniques Discussions

208 little impact from the assimilation until 22 UTC, and then the RMS difference for the
209 MYJ analysis more than doubles whereas it decreases by roughly half for MYNN. The
210 forecasts for the 2 schemes show about the same differences with the sonde moisture pro-
211 files throughout the day. The U-velocity profiles (c) begin to show differences between
212 the MYJ and MYNN by 8 UTC (3 a.m. local time) and the assimilation reduces the RMS
213 differences with sonde profiles significantly by 22 UTC for both models. The V-velocity
214 profiles (d) begin to differ between MYJ and MYNN for the forecasts at 8 UTC, and as-
215 similation reduces the RMS differences with sondes in late afternoon by 10-20%.

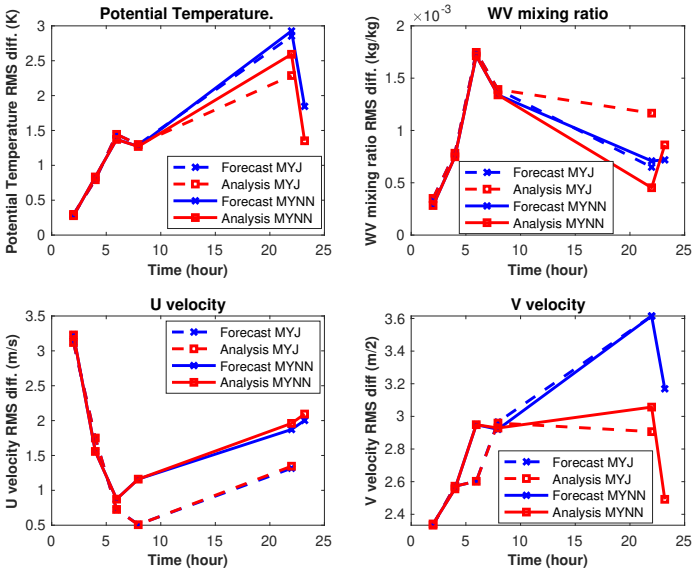

Figure 2. RMS difference from surface to top of PBL vs. time of forecast (blue) and analysis (red) with sonde profiles for (a) potential temperature, (b) water vapor, (c) zonal velocity and (d) meridional velocity. The solid lines are for the MYNN PBL model and the dashed lines are for the MYJ PBL model. Times shown are UTC.

216 We would like to understand why there is no data impact during night time and
217 early morning, whereas there is overall improvement in the late afternoon. To this end,
218 we plot the forecast, analysis and sonde profiles (T, Q, U and V) at 4 UTC (11 p.m. lo-
219 cal time) and 22 UTC (5 p.m. local time) in Figures 3-6. At 4 UTC, (Figures 3,4) these
220 clearly indicate that there is no correction made by the assimilation, as the red and plue

https://doi.org/10.5194/amt-2020-238
Preprint. Discussion started: 7 July 2020


Atmospheric Measurement Techniques Discussions

profiles coincide. But it also shows that the profiles (particularly temperature and moisture) accurately follow the sonde profiles, meaning that there is little room for improvement to the forecast state. This is consistent with the PBLH forecasts in Figure (1), which shows that little difference between the forecast (particulary MYJ) and lidar observation is very small. In the late afternoon (Figures 5, 6) show that there are large differences forecast between the forecast and sonde profiles for all of the state variables, and the forecast PBLH values differ substantially from the lidar measurements as well. The correction to to the profiles is generally in the correct direction, indicating that the forecast error covariance from the ensemble can relate the PBLH to the state variables. So the forecasts that accurately predicted both PBLH and state variable profiles in the early morning were not corrected, while the less accurate afternoon forecast was drawn towards the independent sonde measurements. The assimilation also made changes to the vertical velocity (W) in the afternoon, but there is no indpendent data to compare with so we have not included it.

Initial experiments without vertical covariance localization (not shown) found that the analysis profiles were changed substantially well into the troposphere, which increased the RMS differences with the sonde profiles there. With the addition of the vertical correlation the analysis profiles relax back to the forecast in the troposphere. The WV profile is shown to be increased by the assimilation (since WV and PBLH are negatively correlated and higher PBLH corresponds to lower WV levels in the PBL models), but the analysis overshoots the sonde WV profile, hence causing the increase in the RMS difference in Figure 2(b). Compared to temperature, WV is highly variable in time and space and it has been shown in the past that slanted balloon trajectories under estimate the WV present (Demoz et al 2006; Crook, 1996). The PBLH may be a macroscale observation that is forcing a correction to the WV flux and hence pointing out an issue in measurements. Future studies should look at the profile measurements of WV from lidars. The two components of velocity (c,d) are both drawn towards the sonde profiles, but by more modest amounts. These analysis profiles in show that, for this one analysis time, the assimilation is pushing the state variables in the proper direction. The reason for these corrections to the state variable profiles is that the error covariance between PBLH and each state variable, $\mathbf{P}^f\mathbf{H}^T$, can be computed from the ensemble of profiles that was collected from the model grid. The forecast PBLH for each profile was computed using the

https://doi.org/10.5194/amt-2020-238
Preprint. Discussion started: 7 July 2020

Atmospheric Measurement Techniques Discussions

253 full PBL physics, and therefore contains the essential correlation information between
254 these variables.

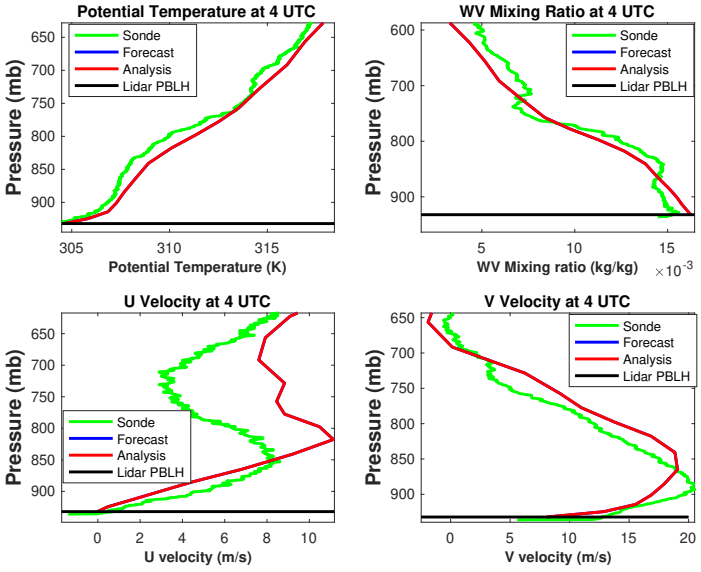

Figure 3. Profiles from sonde (green), forecast (blue) and analysis (red) for potential temperature, water vapor mixing ratio, u-velocity and v-velocity at 4 UTC, July 11, 2015 in Greensburg, KS. The model uses the MYJ physics parameterization.

255 The increasing differences between the PBLH and profile forecasts from early morn-
256 ing to late afternoon only partly explain the much larger impact of the assimilation at
257 22 UTC. We can also analyze this by plotting the error covariance between PBLH and
258 each of the state variables, seen in Figure 7 at different times during the day. The co-
259 variance with temperature (a) is always positive, and grows by a factor of 4 by late af-
260 ternoon near the surface. The covariance with WV is mostly negative and grows by roughly
261 a factor of 5, while the covariance with the two components of velocity oscillate between
262 positive and negative and shows less consistent growth. Thus, the most significant im-
263 pact of assimilation to temperature and moisture occur in late afternoon while more lim-
264 ited velocity corrections are largely constrained by the correlations determined by the
265 ensemble of model forecast states.

https://doi.org/10.5194/amt-2020-238
Preprint. Discussion started: 7 July 2020

Atmospheric Measurement Techniques Discussions
Open Access
EGU

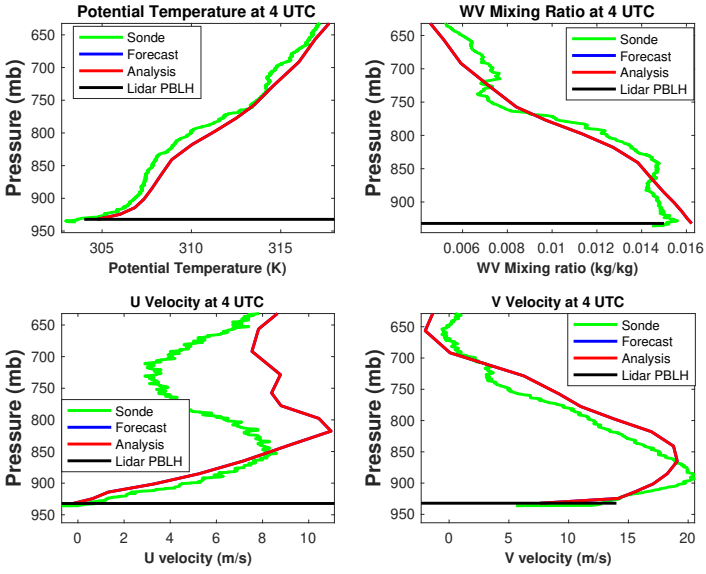

Figure 4. Same as figure 3 except using MYNN model.

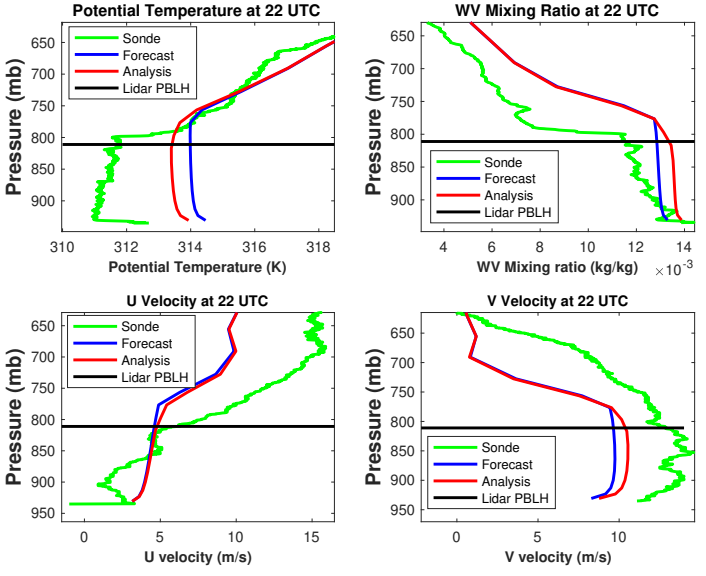

Figure 5. Same as figure 3 except using except at time 22 UTC.

https://doi.org/10.5194/amt-2020-238
Preprint. Discussion started: 7 July 2020

Atmospheric Measurement Techniques Discussions

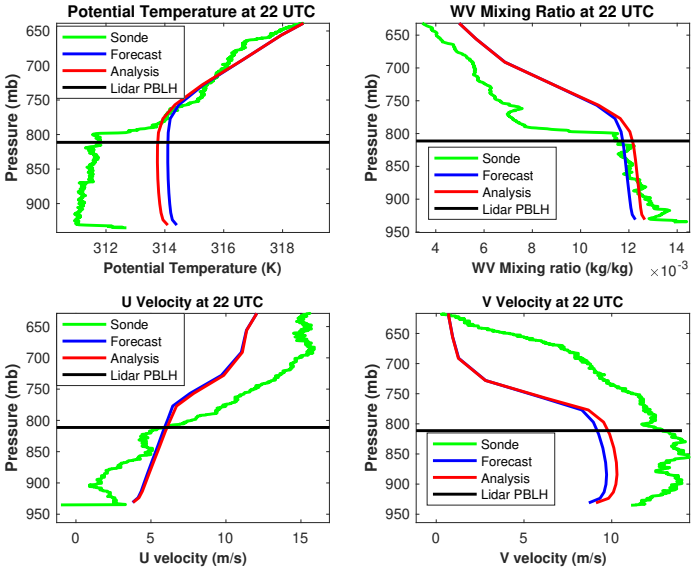

Figure 6. Same as figure 5 except using MYNN model.

4 Conclusions

These offline data assimilation experiments indicate that assimilation ground based lidar backscatter and wind measurements of PBLH into a regional NWP model will likely lead to significant improvements within the PBL, particulary when this approach is applied to an EnKF assimilation system with cycling. Using two NU-WRF forecasts over a period of one day with different PBL physics models, we show how the state variables, T, WV, U and V can be corrected using an an assimilation system with ensemble based error covariances. During the night and early morning the assimilation has little or no impact on the state variables, but by late afternoon the temperature field is drawn closer to independent sonde measurements. We have shown that the lack of data impact early in the day is the due to the high accuracy of the model and lack of correlation between the forecast PBLH and temperature profiles at that time. Later in the day, when the model is less accurate in predicting the growth of the boundary layer, the data begins to draw the analysis towards the independent sonde profiles. The water vapor mixing ratio is over corrected in the direction of sonde data, and this could likely be tuned in an assimilation system. The assimilation corrected the two velocity components by smaller amounts, but still reduced differences with the sonde profiles. These corrections are the result of

https://doi.org/10.5194/amt-2020-238
Preprint. Discussion started: 7 July 2020

Atmospheric Measurement Techniques Discussions

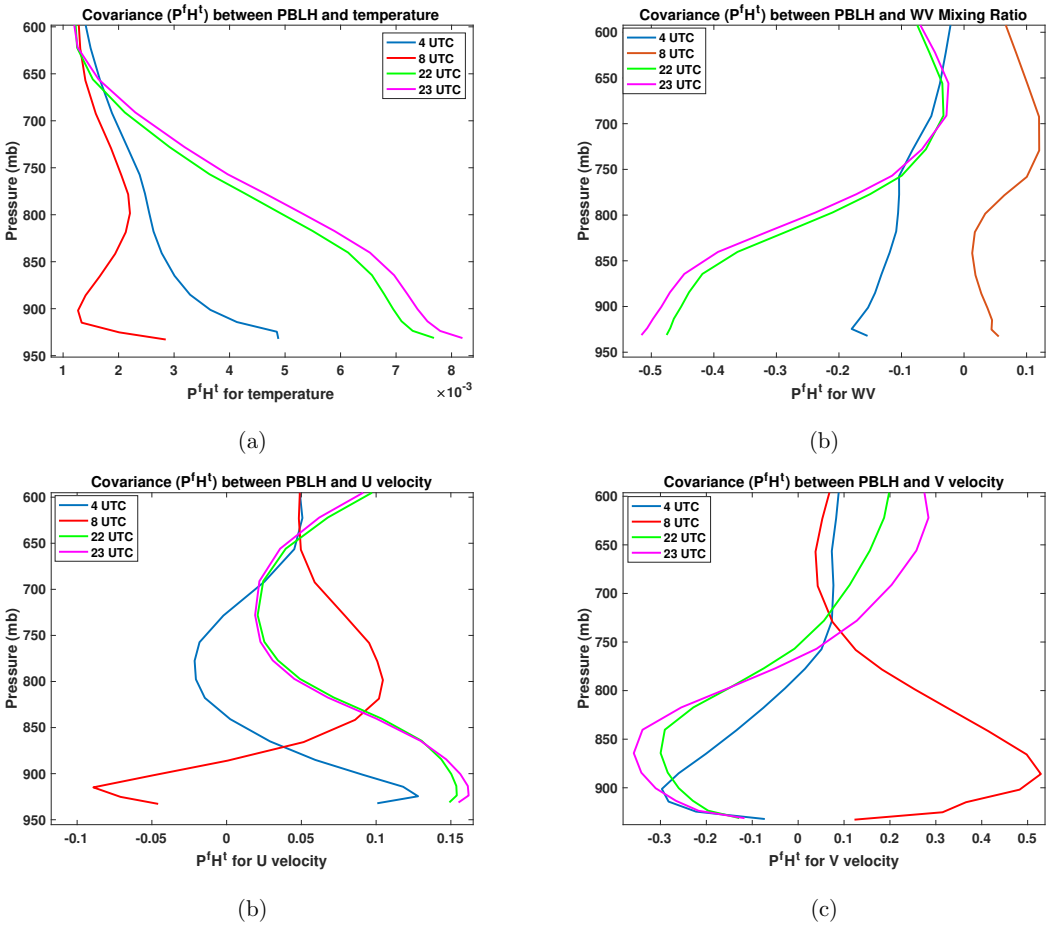

Figure 7. Covariance $\mathbf{P}^f\mathbf{H}^T$ between PBLH and temperature (a), water vapor (b), U-velocity (c) and V-velocity (d), at times 4, 8, 22 and 23 UTC, for PBL physics model MYHH.

https://doi.org/10.5194/amt-2020-238
Preprint. Discussion started: 7 July 2020


Atmospheric Measurement Techniques Discussions

ensemble computed error covariances between the PBLH and the state variable profiles within the PBL. The results here indicate that this approach could be used in a forecast system in a way that that the PBLH observational information could be carried forward in time so as to improve the forecast accuracy within the PBL. An additional value of assimilating PBLH is its close connection with the PBL scheme used in the model. The covariances between PBLH and the different state variables through the PBL physics scheme. This has an impact on the corrections made to the profiles within the PBL, which can be used as another way to evaluate the physics parameterizations. For example, the MYJ and MYNN result in analysis profiles that differ, though a full evaluation would require that the assimilation be implemented into a cycling data assimilation system.

This work is intended only to demonstrate a necessary first step in terms of how ensemble statistics can help to constrain profiles within the PBL by assimilating PBLH observations. A more complete demonstration of this approach will require the construction of an EnKF, and run over many days with a variety of weather patterns, including significantly warmer(cooler) and wetter(drier) days. This is needed to show how the assimilated PBLH observations will impact future forecasts within the PBL. The PBLH assimilation withn the EnKF framework could be done in any of numerous existing enKF assimilation systems that connect with WRF, including NU-WRf (Lidard-Peters *et al.*, 2015) and WRF-DART (Anderson *et al.*, 2009).

5 Acknowledgments

B. Demoz was funded by National Science Foundation award (AGS-1503563) to the University of Maryland, Baltimore County and through NOAA Cooperative Science Center in Atmospheric Sciences and Meteorology, funded by the Educational Partnership Program at NOAA in collaboration with Howard University.

6 Data Sets

PECAN (`https://data.eol.ucar.edu/master_list/?project=PECAN\verb`) data are archived by NCAR/EOL, which is funded by NSF. The forecast and analysis fields produced for this work are stored at https://alg.umbc.edu/pecan/.

https://doi.org/10.5194/amt-2020-238
Preprint. Discussion started: 7 July 2020

Atmospheric Measurement Techniques Discussions

7 Competing Interests

The authors declare that they have no conflict of interest.

8 Author Contributions

Andrew Tangborn built the assimilation system, with input from Jeffrey Anderson on the algorithm. Belay Demoz and Brian Carroll provided the lidar observations. Joseph Santanello provided background information on PBL physics. All of the authors contributed to writing and revising the paper.

9 References

Anderson, J.L., T. Hoar, K. Raeder, H. Liu, N. Collins, R. Torn and A. Arellano (2009), The Data Assimilation Research Testbed: A Community Facility, *Bull. Amer. Met. Soc.*, 90, 1283-1296 doi:10.1175/2009BAMS2618.1.

Ao, C.O., T. K. Chan, B. A. Iijima, J.-L. Li, A. J. Mannucci, J. Teixeira, B. Tian, and D. E. Waliser (2008), Planetary boundary layer information from GPS radio occultation measurements, *Proceedings of GRAS SAF Workshop on Applications of GPSRO Measurements*, ECMWF, Reading, UK.

Banks, R. F., J. Tiana-Alsina, F. Rocadenbosch, and J. M. Baldasano (2015) Performance evaluation of the boundary-layer height from lidar and the Weather Research and Forecasting Model at an urban coastal site in the north-east Iberian Peninsula. *Bound.-Layer Meteor.*, 157, 265–292, https://doi.org/ 10.1007/s10546-015-0056-2.

Bonin, T.A., B.J. Carroll, R.M. Hardesty, W.A. Brewer, K. Hajney, O.E. Salmon and P.B. Shepson (2018), Doppler Lidar Observations of the Mixing Height in Indianapolis Using an Automated Composite Fuzzy Logic Approach, *J. Atmos. Ocean Tech.*, 35, 473-490.

Browning, K. A., and Coauthors (2007), The Convective Storm Initiation Project. , *Bull. Amer. Meteor. Soc.*, 88, 1939–1955, https://doi.org/10.1175/BAMS-88-12-1939.

https://doi.org/10.5194/amt-2020-238
Preprint. Discussion started: 7 July 2020

Atmospheric Measurement Techniques Discussions

Carroll, B. J., Demoz, B. B., and Delgado, R. (2019). An overview of low-level jet winds and corresponding mixed layer depths during PECAN. Journal of Geophysical Research: Atmospheres, 124(16), 9141-9160. https://doi.org/10.1029/2019JD030658.

Cohen, A.E., S.M. Cavallo, M.C. Coniglio and H.E. Brook (2015), A Review of Planetary Boundary Layer Parameterization Schemes and Their Sensitivity in Simulating Southeastern U.S. Cold Season Severe Weather Environments, *Wea. Forecat.*, 30, 591-612.

Delgado, R., Carroll, B. and Demoz, B. (2016). FP2 UMBC Doppler Lidar Line of Sight Wind Data. Version 1.1 [Data set]. UCAR/NCAR - Earth Observing Laboratory. Accessed 29 May 2017. https://doi.org/10.5065/d6q81b4h.

Evensen, G. (2009), *Data assimilation: the ensemble Kalman filter*, Springer.

Geerts, B., and Coauthors, (2017), The 2015 Plains Elevated Convection At Night field project. *Bull. Amer. Meteor. Soc.*, 98, 767–786, https://doi.org/10.1175/BAMS-D-15-00257.1.

Hegarty, J.D., J. Lewis, E.L. McGrath-Spangler, J. Henderson, A.J. Scarino, P. DeCola, R. Ferrare, M. Hicks, R.D. Adams-Selin and E.J. Welton (2018) Analysis of the Planetary Boundary Layer Height during DISCOVER-AQ Baltimore–Washington, D.C., with Lidar and High-Resolution WRF Modeling, *J. Appl. Meteo. Climat.*, 57, 2679-2696.

Hicks, M., D. Atkinson, B. Demoz, K. Vermeesch and R. Delgado (2016), The National Weather Service Ceilometer Planetary Boundary Layer Project, *The 27th International Laser Radar Conference (ILRC 27)*, https://doi.org/10.1051/epjconf/201611915004.

Hicks, M., B. Demoz, K. Vermeesch and D. Atkinson (2019), Intercomparison of Mixing Layer Heights from the National Weather Service Ceilometer Test Sites and Collocated Radiosondes, *J. Atmos. Ocean Tech.*, 36, 129-137.

Hong, S.-Y. and H.-L. Pan (1996), Nonlocal boundary layer vertical diffusion in a medium-range forecast model, *Mon. Wea. Rev.*, 124, 2332-2339.

Hong, S.-Y. and H.-L. Pan (1998), Convective Trigger Function for a Mass-Flux Cumulus Parameterization Scheme, *Mon. Wea. Rev*, 126, 2599-2620.

https://doi.org/10.5194/amt-2020-238
Preprint. Discussion started: 7 July 2020

Atmospheric Measurement Techniques Discussions

Janjic, Z.I. (1994), The Step-mountain eta coordinate model: Further developments of the convection, viscous sublayer, and turbulence closure, *Mon. Wea. Rev.*, 122, 927-945.

Janjic, Z.I. (2002), Nonsingular Implementation of the Mellor-Yamada Level 2.5 Scheme in the NCEP Meso model (NCEP Office Note No. 437).

T. N. Knepp, J.J. Szykman, R. Long, R. M. Duvall, J. Krug, M. Beaver, K. Cavender, K. Kronmiller, M. Wheeler, R. Delgado, R. Hoff, T. Berkoff, E. Olson, R. Clark, D. Wolfe, D. Van Gilst, D. Neil (2017), Assessment of mixed-layer height estimation from single-wavelength ceilometer profiles, *Atmos. Meas. Tech.*, 10, 3963-3983.

Mellor, G.L. and T. Yamada (1974), A Hierarchy of Turbulence Closure Models for Planetary Boundary Layers, *J. Atmos. Sci.*, 31, 1791-1806.

Mellor, G.L. and T. Yamada (1982), Development of a turbulence closure model for geophysical fluid problems, *Rev. Geophys.*, 20, 851-875.

Nakashini, M. and H. Niino (2009), Development of an improved turbulence closure model for the atmospheric boundary layer, *J. Met. Soc. Japan*, 87, 895-912.

National Research Council (2009), Observing Weather and Climate from the Ground Up: A Nationwide Network of Networks, in: Observing Weather and Climate from the Ground Up: A Nationwide Network of Networks, 1–234, Natl. Academies Press, 2101 Constitution Ave, Washington, DC 20418 USA.

NCAR Technical Note (2012), Thermodynamic Profiling Technologies Workshop Report to the National Science Foundation and the National Weather Service, National Center for Atmospheric Research.

Oke, P.R., G.B. Brassington, D.A. Griffin, and A. Schiller (2010), Ocean data assimilation: a case for ensemble optimal interpolation, *Austr. Meteor.Ocean. J.*, 59, 67-76.

Peters-Lidard, C.A. and Co-authors (2015), Integrated modeling of aerosol, cloud, precipitation and land processes at satellite-resolved scales, *Environ. Mod. Soft.*, 67, 149-159.

https://doi.org/10.5194/amt-2020-238
Preprint. Discussion started: 7 July 2020

Atmospheric Measurement Techniques Discussions

389 Santanello, J.A. and Co-authors (2018), Land–Atmosphere Interactions: The LoCo Per-
390 spective, *Bull. Amer. Meteor. Soc*, https://doi.org/10.1175/BAMS-D-17-0001.1.

391 Santanello, J.A.,, S.Q. Zhang, D.D. Turner, P. Lawston, and W.G. Blumberg, PBL Ther-
392 modynamic Profile Assimilation and Impacts on Land-Atmosphere Coupling, AGU Fall
393 Meeting, San Francisco, CA, Dec. 9-13, 2019.

394 Tucker, S.C., S.J. Senff, A.M. Weickmann, W.A. Brewer, R.M. Banta, S.P. Sandberg,
395 D.C. Law and R.M. Hardesty (2009), Doppler Lidar Estimation of Mixing Height Us-
396 ing Turbulence, Shear, and Aerosol Profiles, *J. Atmos. Ocean Tech.*, 26, 673-688.